Title
Polymictic pool behavior in a montane meadow, Sierra Nevada, CA

Author
Lucas, Ryan

Publication Date
2016-04-01

Peer reviewed

Polymictic pool behavior in a montane meadow, Sierra Nevada, CA

by
Ryan G. Lucas[1,2]*, Francisco Suárez[3], Scott W. Tyler[4], Jean E. Moran[5], and, Martha H. Conklin[1,6]
DOI: 10.1002/hyp.10834

[1]Sierra Nevada Research Institute, [2]Environmental Systems Graduate Group, and, [6]School of Engineering
University of California, Merced, CA
5200 North Lake Road, 95343, USA.

[3] Department of Hydraulic and Environmental Engineering
Pontificia Universidad Católica de Chile
Avda. Vicuña Mackenna 4860, Santiago, Chile

[4]Geological Sciences and Engineering
University of Nevada, Reno
1664 N. Virginia Street, Reno 89557, USA

[5]Earth and Environmental Sciences
California State University, East Bay
25800 Carlos Bee Boulevard, Hayward, CA 94542, USA

*Corresponding author: Ryan Lucas
Present Address: University of California, Merced, CA, 5200 North Lake Road, 95343,
Email: rlucas@ucmerced.edu; Phone: (805) 680-0903

Authors have no conflict of interest to declare.

Keywords: Stream Pool Stratification; Meadow Hydrology; Sierra Nevada Meadows, Dissolved Organic Carbon

ABSTRACT

We observed polymictic behavior in stream pools in Long Meadow, Sequoia National Park, California—part of the Southern Sierra Critical Zone Observatory. Stream pools stratified thermally during the day time and were isothermal at night—this pattern persists from the middle of summer into the fall. We found that four characteristics typical of a mountain meadow environment—low stream flow, open sky, cold groundwater discharge, and elevated organic carbon concentrations—are particularly conducive to pool stratification. Incoming shortwave radiation was the dominant energy input to heat pool water while nighttime emitted longwave radiation was the major cooling mechanism. Relatively cold groundwater discharge into the pool bottom increased density stratification within the pool. Elevated DOC concentrations increased the capacity of the pool to absorb photosynthetically active radiation and also promoted stratification. Stream velocities in the meadow were generally insufficient to meet threshold Richardson numbers and mix the pools during the daytime; smaller stream cross sectional areas would have potential for destabilizing pools in the daytime. We propose a conceptual model for describing polymictic stream pools and assessing the potential for polymictic pools to occur.

INTRODUCTION

Stream pools are a distinctive feature of many stream systems; they are particularly prevalent in mountain streams in pool-riffle and step pool structures (Whitaker, 1982; Chartrand and Whiting, 2000). Stream pools tend to have lower stream velocity and a depressed channel as compared to riffles (Whitaker, 1982; Lisle, 1987; Chartrand and Whiting, 2000). Many studies focus on stream pools as refugia for fish and other organisms (Lisle, 1987; Bormans and Webster, 1998; Tate *et al.*, 2007; Matthews *et al.*, 1994; Matthews and Berg, 1997; Nielsen *et al.*, 1994; O'Donnell 2012). Thermal stratification of stream pools—driven by radiative and sensible heat fluxes warming the surface of the water body and resulting in a density discrepancy between layers of different water temperature—is well documented (Bormans and Webster, 1998; Tate *et al.*, 2007; Matthews *et al.*, 1994; Matthews and Berg, 1997; Nielsen *et al.*, 1994; O'Donnell 2012). The buoyant forces created by the density discrepancy are opposed by turbulent mixing and entrainment incurred from stream flow into the pools.

Bormans and Webster (1998) investigated thermal stratification in low flow rivers in Australia. The pools they investigated were relatively large (35-40 km long, 40-110 m wide, and up to 6 m deep) compared to pools studied in the western United States (2-10 m diameter, and up to 5 m deep (Tate *et al.*, 2007; Matthews *et al.*, 1994; Matthews and Berg, 1997; Nielsen *et al.*, 1994; O'Donnell 2012)). Bormans and Webster (1998) found that stratification in their pools was predominantly a function of net energy flux (solar radiation, sensible and latent heat fluxes) and stream flow. Low stream flow combined with high net energy flux at the pool surface produced stable pools that remained stratified. As stream flow increased and net surface energy flux decreased, stability decreased and pools mixed daily or remained mixed for extended periods. Studies of stream pool stratification in the western US were conducted in highly varied systems, from a stream in southern California (Matthews and Berg, 1997), to the central Sierra Nevada Mountains (Mathews *et al.*, 1994), the northern California coast (Nielsen *et al.*, 1994), northeastern California (Tate *et al.*, 2007), and Oregon (O'Donnell, 2012), and typically focused on salmonid use of thermally stratified pools as thermal refugia. Tate *et al.* (2007) studied two pools at 1,400 m elevation that exhibited seasonal stratification. Nielsen *et al.* (1994) proposed that thermally stratified stream pools occur where there is a significant cold water input into the bottom of the pool and where turbulent mixing from stream flow is minimized—the pool may be in a side channel, protected by a channel feature such as a gravel bar or large woody debris, or may exist where stream flow is very low. Matthews *et al.* (1994) monitored pool temperatures at various depths in a Sierra Nevada Mountain stream and the preferential use of cold zones by trout; however, their study did not explain the mechanisms that drove thermal stratification of the stream pools. While these mechanisms for stratification are consistently mentioned in the literature, the surface energy budget, effect of stream velocity, and cold water input to the pool bottom have not been quantified in a way that determines the conditions that lead to and maintain stratification.

While energy fluxes across the pool surface, stream flow, and the influence of cold water inflow have been characterized in stream pool stratification studies as noted above (Bormans and Webster, 1998; Tate *et al.*, 2007; Matthews *et al.*, 1994; Matthews and Berg, 1997; Nielsen *et al.*, 1994; O'Donnell 2012), in this study we also include the organic carbon concentration in the pool to constrain solar energy absorption in the water column. In addition to water itself, organic matter is a major light absorbing component of natural aquatic systems (Kirk, 1994). Organic matter in the water column comes from soluble humic substances leached from the soil and from the decomposition of plant matter in the water column. The latter may be especially significant in highly productive waters.

In Long Meadow, Sequoia National Park, we observed meadow pools following a polymictic pattern, stratifying thermally during warm daytime hours and mixing completely during cooler nighttime hours. We have observed stream pools in several meadow systems in the Sierra Nevada though the existence of stream pools in meadow systems is not well documented. Meadows of the Sierra Nevada Mountains, California, tend to lie in low gradient, groundwater fed areas (Ratliff, 1985). Montane meadows are typically drained by a stream, serve as riparian wetlands critical in connecting land and aquatic systems (Purdy and Moyle, 2006), and play an important role in the transfer of water, energy, organic matter, and nutrients (Kattelmann and Embury, 1996).

The purpose of this study is to understand the processes that drive thermal stratification in mountain meadow pools. Understanding these processes allows quantification of the impacts of pool stratification on surface water residence times, and on the transfer of energy, organic matter and nutrients. Our aim is to provide a conceptual model that could be used in a general way, to determine the factors that drive polymictic pool behavior. In this study we use physical measurements gathered over the course of two summers to monitor pool behavior in Long Meadow, Sequoia National Park, California. We discuss the factors that drive pool stratification and the ways in which the meadow environment provides favorable conditions for polymictic pool behavior.

METHODS

Site Description

This study was conducted in Long Meadow, Sequoia National Park, California (118.7373° W, 36.5927° N). Long Meadow is approximately 1.5 km long, up to 100 m wide (Figure 1) and slopes from south to north at an approximate 4% grade. The meadow lies in a glaciated valley within the Wolverton Creek catchment at approximately 2,200 m above mean sea level. The meadow soil is described as a frigid Aquept characterized by several centimeters of highly organic soil underlain by coarse sandy loam and very dark grey coarse sandy loam (Huntington and Akeson, 1987). The soil is underlain by granodioritic alluvium up to 30 m in thickness (Wahrhaftig *et al.*, 1984). Vegetation in the meadow is dominated by wet meadow grasses and sedges with pockets of lodegepole pine and willow. The meadow basin is constrained by granodioritic bedrock to the south, west and east, and by a glacial moraine and Wolverton Creek to the north (Wahrhaftig *et al.*, 1984). The soils associated with the hill slopes around the meadow are comprised of loamy coarse sands and coarse sandy loams characterized as Lithic Xerumbrepts and Pachic Xerumbrepts (Huntington and Akeson, 1987). Vegetation on these hills consist of Red Fir, Jeffery Pine and Lodgepole Pine Forests, as well as wet meadow, meadow and willow shrub land, Manzanita and Ceonothus shrubs, and upland herbaceous plants (National Park Service Vegetation Inventory Project, 2014).

Surface water input to the meadow is supplied by two ephemeral streams, and surface water in the meadow flows at times in a poorly defined stream channel punctuated by several pools. The meadow stream runs intermittently in both space and time; the stream channel is not identifiable in some areas of the meadow. At least ten stream pools are present through the length of the Long Meadow. Stream pools, up to 1.3 m deep—measured from the meadow surface to the bottom of the pool, 1 m wide, and 1 to 4 m long, are present along both well and poorly defined stream channel reaches of the meadow. Sheet flow over the surface of the meadow occurs during snowmelt when surface flow is not confined to the stream channel. By late summer, surface water flow is discontinuous longitudinally in the meadow and the meadow pools are hydrologically isolated from surface water as the water level drops—the level of the pool surface is maintained by the height of the groundwater table. The narrow meadow is shaded by the adjacent conifers only in the early morning and late afternoon— and groundwater discharge persists in the center of the meadow through the warm summer months.

For this study, we discuss a single pool—identified as LP-33 (named after the adjacent lodgepole pine tree)—in detail. LP-33 is 1.3 m deep—measured from the meadow surface to the bottom of the pool, approximately 1 m at its widest point and 2 meters long. The pool is located near the center of the meadow (Figure 1).

Physical measurements

Pool vertical temperature profiles in the LP-33 pool were measured using Onset HOBO TidbiT v2 temperature loggers (Onset, Bourne, MA). The TidbiT temperature loggers were attached to a bamboo ski patrol stake at 15-20 cm intervals and the stake was placed at the approximate center of LP-33. These loggers were programmed to measure temperature at five minute intervals and collected data from July 11, 2008 to September 10, 2008, and during a follow up deployment, from July 15, 2009 to October 13, 2009. Meadow stream temperatures were measured from July 7-11, 2008 using a fiber optic distributed temperature sensor (DTS) as described by Tyler *et al.* (2009) and Selker *et al.* (2006). We utilized a Sensornet Sentinal-DTS (Sensornet, Hertfordshire, UK) system with 2 m spatial resolution integrating measurements over 2 minute time intervals over 1,000 m of fiber-optic cable placed in the meadow system. The DTS measurements have ±0.01 °C precision and ±0.1 °C accuracy when integrating over a 2 minute time interval based upon analysis following Hausner *et al.* (2011). Pool water temperatures and electrical conductivity were measured in the field using a hand held meter (YSI 30M, YSI Inc., Yellow Springs, OH).

Wolverton meteorological station (Figure 1), located 270 m from the meadow is equipped to measure air temperature and relative humidity (HMP-45AC , Campbell Sci., Logan, UT), wind speed and direction (Young 5103 Anemometer, R. M. Young Co., Traverse City, MI), net radiation (NR Lite , Kipp & Zonen, Delft, The Netherlands), and barometric pressure (Barologger Gold, Solinst, Georgetown, ON, Canada). A micrometeorological station deployed in the meadow from July 6-12, 2008 measured air temperature and relative humidity (CS215, Campbell Sci., Logan, UT), wind speed and direction (Young 8100 3D sonic anemometer, R. M. Young Co., Traverse City, MI), and radiation (CNR4, Kipp & Zonen, Delft, The Netherlands). Net radiation is plotted for both the Wolverton meteorological station and the micrometeorological station in Figure 2—this figure highlights the shading effect of the forest around the Wolverton station. Incoming longwave radiation was measured in 5 additional meadows in the Sierra Nevada with a 4-component radiometer (NR-01, HuksefluxUSA, Manorville, NY).

Hydraulic head and groundwater temperature were recorded in six piezometer clusters in the meadow (Figure 1). The three piezometers located north of LP-33 are referred to as the SM cluster. Each piezometer cluster consisted of deep (1.7 m depth), mid (1.2 m depth), and shallow (0.70 m depth) piezometers. After the pools are disconnected due to stream flow cessation, water levels in the pools are maintained as a function of the groundwater table elevation, as noted above. The piezometers were constructed with 5 cm of 0.010 inch slotted screen; the remainder of the conduit is blank casing. Pressure transducers (Levelogger Gold, Solinst, Georgetown, ON, Canada) suspended in the piezometers recorded hydraulic head and temperature at 15 minute intervals.

Photosynthetically active radiation (PAR) was measured in the water column in Top Pool (Figure 1) using a spherical quantum sensor (LI-193, LI-COR, Inc., Lincoln, NE). Measurements were taken just below the surface of the pool and at 10, 25, 50, 75, and 100 cm depth. PAR measurements were collected between 9:00 am and 12:00 pm PST on September 25, 2015.

Stream velocity profiles were measured using an Acoustic Doppler Velocimeter (Flowtracker Handheld-ADV, Sontek/Xylem, Inc., San Diego, CA). Stream cross sections were delineated at the SMLL stream site using a laser level; these are presented in Figure 3. Stream discharge rates were obtained by combining the velocity measurements and the cross section information; additional stream discharge measurements were determined via constant rate tracer (salt) tests (Dingman, 2015). The mean stream velocity was calculated by dividing the discharge rate by the stream cross sectional area.

Water sampling

During the 2008 deployment, water samples were collected at various locations in the meadow and Wolverton Creek. One of the 13 monitoring wells in the meadow produced enough water for sample collection. The location of this well (termed "Meadow Well") is indicated in Figure 1. The Meadow Well is 2.15 m deep and is screened from 0.32 to 2.15 m below ground surface with 0.010 inch slotted screen. Samples collected during the deployment were analyzed at Lawrence Livermore National Laboratory for dissolved organic carbon (DOC), and Radon-222 activity. Forty mL samples were filtered in the field at 0.45 µm, collected in amber VOA vials with no headspace and stored at 4 °C until analysis for DOC. DOC concentrations were measured with an OI Corporation Model 1030 wet chemical oxidation TIC/TOC analyzer and are reported in units of milligrams per liter (mg L^{-1}) as C. The analytical uncertainty is less than or equal to 0.3 mg L^{-1} for DOC concentrations. Water samples for Radon-222 analysis were collected by injecting 10 mL of water into a scintillation vial containing 10 mL of a mineral oil cocktail using a syringe with a curved tip. This technique allows for minimal degassing of Radon from the sample and rapid analysis by decay counting. Radon activities in water samples were measured within three days of sampling using a Quantalus 1220 liquid scintillation counter. The detection limit for Radon-222 is 20 pCi L^{-1} and analytical uncertainty is less than or equal to 10%.

Calculations

Net solar radiation for times when the micrometeorological station was not deployed and emitted long wave radiation (LW_{emi}) were calculated using methods described by Allen *et al.* (1998). Sensible and latent heat fluxes across the pool surface were calculated for July 11, 2008; this was the only day that both the micrometeorological station and the pool temperature loggers were deployed. Sensible and latent heat fluxes were calculated using (Fischer *et al.*, 1979):

(1) $$H = C_s \rho_A C_p U (T_o - T)$$

(2) $$LE = C_e \rho_A L_w U (Q_o - Q)$$

where H is the sensible heat flux across the pool surface, C_s is the sensible heat flux transfer coefficient, ρ_A is the density of air, C_p is the specific heat of air, U is wind speed, T_o is the water surface temperature measured by the temperature logger nearest to the pool surface, and T is the air temperature measured at the micrometeorological station. LE is the latent heat flux, C_e is the latent heat flux transfer coefficient, L_w is the latent heat of vaporization, Q_o is the saturation specific humidity at the air-water interface, and Q is the specific humidity of air. It is common to assume that $C_s \approx C_e$. Hicks (1972) suggests $C_s = 1.45 \cdot 10^{-3}$ for a neutrally stable boundary layer. Use of constant bulk transfer coefficients are not recommended for diel time scales and atmospheric stability should be taken in to account (MacIntyre *et al.*, 2002). MacIntyre *et al.* (2002) calculated bulk transfer coefficients for an embayment in Lake Victoria ragning from $1.1 \cdot 10^{-3}$ to $4.0 \cdot 10^{-3}$. We used this range to constrain sensible and latent heat fluxes by calculating each with the lower and upper bounds of the range presented in MacIntyre *et al.* (2002). The small dimensions of the pool may result in a less than fully formed thermal or momentum boundary layer; in that case the use of bulk transfer coefficients may not be appropriate. Latent heat flux that includes both wind-forced and free convection was calculated using the expression developed by Adams *et al.* (1990):

(3) $$LE = \left[\left(\lambda (T_{wv} - T_{av})^{1/3} \right)^2 + (5.1 \cdot 10^{-2} A^{-0.05} U)^2 \right]^{1/2} \cdot (e_{sw} - e_a)$$

where LE is the latent heat flux from both forced wind convection and free convection, λ is a constant equal to $2.7 \cdot 10^{-2}$ W m^{-2} Pa^{-1} $(^{\circ}C)^{-1/3}$, T_{wv} is the virtual temperature of the surface water, T_{av} is the virtual temperature of air at 2 m, A is the surface area of the pool, e_{sw} is the saturation vapor pressure at the air-water interface, and e_a is the vapor pressure in the ambient air.

Vertical Darcy flux was calculated using data from the clustered piezometer data and Darcy's Law:

(4) $$q = -K_s \frac{dH}{dz}$$

where q is the Darcy flux, K_s is the soil saturated hydraulic conductivity, dH is the difference in hydraulic head and dz is the vertical distance between piezometers pairs. K_s was determined by conducting slug tests in monitoring wells associated with each piezometer cluster and using the Hvorslev method (Fetter, 1994)—slug tests were conducted by evacuating the wells and measuring the recovery to the static water level.

We calculated the Richardson number as a function of stream flow velocity (R_{is}):

(5) $$R_{is} = \frac{g' z}{U^2}$$

where $g' = g\,\Delta\rho/\rho_o$, g is gravity (m s^{-2}), $\Delta\rho$ is the density discrepancy between layers (kg m^{-3}), ρ_o is the reference density (kg m^{-3}), z is depth (m) from the pool surface to the bottom of the mixed layer and U is the horizontal stream velocity.

RESULTS

Data from the DTS indicated that pools located near the meadow margin had average temperatures similar to the stream whereas temperatures in pools in the middle sections of the meadows were lower than the stream temperatures (Fig. 4 b-e). Measurements from the handheld meter were used to identify vertical thermal stratification in pools located in the middle section of the meadow; temperature differences were also measured horizontally across the bottom of the pools, suggesting localized influence of groundwater. Specific conductivity did not vary sufficiently in the vertical to modify the density stratification. Temperatures measured in coils of fiber at the bottom and approximately mid depth of the Top Pool—located at the terminal end of the DTS fiber (966 m)—are presented in Figure 2(f). Temperature discrepancies (as determined by DTS results) between the pool temperature and stream temperature measured upstream ranged from a fraction of a degree (C) at the pool located at distance 157 m to 5 ˚C in LP-33 at distance 252 m. The duration of the temperature discrepancies were also variable. The pool at 157 m distance was warmer than the upstream temperature for most of the duration of the DTS deployment. Only in the afternoon on July 11 does this pool exhibit cooler temperatures than the upstream water. LP-33 pool exhibits cooler temperatures than the upstream waters for most of the daylight hours. Greater discrepancies between pool and upstream temperatures are observed in all four pools displayed in Figure 4(b-e) on July 11 than on July 10. In Top Pool, the mid-depth DTS coil warmed up more during the daytime hours than the coil at the bottom of the pool; the mid-depth coil also cooled more to a slightly lower temperature at night than the coil at the bottom of the pool

Time series temperature measurements in LP-33 indicated that the pool was polymictic on all sampling days (Figure 5a,b). During summer, temperatures near the surface tended to exceed 20°C whereas temperatures at the sediment-water interface were 12°C. In early fall, temperatures near the surface initially exceeded 15°C and decreased into October along with near bottom temperatures. In summer, temperatures in the pools became isothermal at night. In fall, inverse thermal stratification developed at night. LP-33 increases in temperature during the day throughout the vertical profile of the pool–at night LP-33 mixes and becomes isothermal (Figure 5c). Stratification begins as air temperature increases in the morning and before net radiation starts to increase (Figure 5c,d). Daily air temperatures are at a minimum (15 ˚C) just before dawn and a maximum (25 ˚C) in the late afternoon; net solar radiation peaks at solar noon (600 W m^{-2}) and is negative at night (Figure 5c).

Incoming shortwave energy was the dominant term in the surface energy budget during the day (Fig. 6a). Heat losses were caused by net long wave radiation and latent heat fluxes (Fig. 6b,d). Sensible heat flux was always a small term with positive values in the day and negative values at night (Fig. 6c). Because of the small fetch associated with the pool, and the dependence of the mass transfer coefficients on atmospheric stability, the exact values of latent heat fluxes are uncertain. The atmosphere over land tends to be unstable during the day; higher values of the mass transfer coefficient may apply when winds are low. Higher wind speeds in the afternoon would likely induce a neutrally stratified boundary layer; mass transfer coefficients would likely be closer to 0.001. Consequently, we infer that latent heat fluxes were generally between 0 and 75 W m^{-2}. Thus, for these ponds, radiative cooling, as indicated by negative net long wave radiation, was the largest component of heat loss. In order for net long wave radiaiotn to be a large heat loss term, incoming long wave radiation must be relatively low. Low values of incoming long wave radiation were measured in and calculated for Long Meadow; these values are of similar magnitude to nighttime incoming longwave radiation values measured in 5 additional Sierra Nevada meadows (Table 1).

Groundwater signals indicate discharge at the meadow center, where LP-33 is located, in both the summer and fall. Groundwater temperatures are 2-5 °C cooler than temperatures measured at the bottom of LP-33. Hydraulic head data indicate that groundwater recharge occurs at the meadow edge in the summer and in the fall. (Table 2). Groundwater discharging into the bottom of LP-33 is consistent with ^{222}Rn results. All samples analyzed for ^{222}Rn activity had detectable levels of ^{222}Rn (data not shown), with higher activities at depth, indicating groundwater discharge (Rogers, 1958; Szabo and Zapecza, 1991; Shaw, 2009). DOC values are generally higher in the meadow locations –meadow pools had an average DOC concentration of 4.83 mg L^{-1}–than in the meadow inlets or in Wolverton Creek. DOC concentrations range from 2.45 mg L^{-1} in Wolverton Creek to 5.25 mg L^{-1} at the meadow outlet (Table 3).

At 12:00 on September 25, 2015, peek PAR measured at the pool surface was 1974 µmol s^{-1} m^{-2}; the minimum PAR measured at 1 m below the surface of the pool was 577 µmol s^{-1} m^{-2}. Underwater PAR measurements at 12:00 on September 25, 2015 indicated an attenuation coefficient, $K_d = 1.2$ m^{-1}. The pools are noticeably brown in color compared to the water flowing in Wolverton Creek.

Stream discharge measured near the SM cluster (Figure 1) site ranged from $1.02 \cdot 10^{-3}$ to $7.84 \cdot 10^{-3}$ m^3 s^{-1}. These measurements correspond to stream velocity ranges of $3 \cdot 10^{-3}$ to $2 \cdot 10^{-2}$ m s^{-1} in the deep channel cross section (Figure 3a) and $1.7 \cdot 10^{-2}$ to $1.3 \cdot 10^{-1}$ m s^{-1} when applied to a shallow channel cross section (Figure 3b). Assuming values for LP-33 at peak stratification on July 10-11, 2008 (Table 4) and stratification is stable for $R_{is} > 0.25$ (Miles 1961, Howard 1961), the associated stream velocity required to breakdown stratification between these layers is $1.27 \cdot 10^{-1}$ m s^{-1} on July 10 and $1.02 \cdot 10^{-1}$ m s^{-1} on July 11, 2008.

DISCUSSION

The DTS deployment in Long Meadow identified 5 anomalies in stream temperature that corresponded with the fiber placement in meadow pools. The pools were anomalously cool during the daylight hours and reflected the stream temperatures during the night. The departure from stream temperature varied, with the largest discrepancy observed in LP-33 pool. Further investigation into pool temperature profiles with a handheld meter showed that these pools exhibited a vertical temperature gradient during daylight hours with the warmest temperatures near the pool surface and the coolest temperatures at the pool bottom. The spatial resolution of the DTS system was limited to 2 m. This resolution was on the same order as the length and width dimensions of the pools and was greater than the depth of the pools. The 2-m resolution of the DTS system was therefore insufficient to detect the spatial variability of pool temperatures during the daytime.

Further investigation into the vertical temperature profile of LP-33 showed that polymictic behavior persisted during summer when air temperatures are warm, the sun angle is high, and stream flow is present in the meadow; this polymictic behavior continues into the fall, when air temperatures are cool, sun angle is lower, stream flow has ceased, pool depth is reduced, and the pool is effectively isolated from surface water flows—though still connected to subsurface processes. In both the summer and fall maximum stratification occurs in the early afternoon between 12:00 and 14:00, when the difference between surface and bottom temperatures is approximately 8 ˚C. In the summer, the pool becomes isothermal at night, while an inverted temperature gradient can occur at night in the fall. Peak incoming shortwave radiation (965 W m^{-2}) measured at the micrometeorological station on July 11, 2008 was nearly three orders of magnitudes greater than the peak sensible heat flux into the pool (~8.5 W m^{-2}), calculated for the same day. Cooling of the pool surface is driven by LW_{emi} (up to 429 W m^{-2}) and *LE* loss (up to 228 W m^{-2}).

Conceptual Model

A conceptual model based on the major parameters discussed in this paper is presented in Figure 9. Pool stratification is driven by energy flux—primarily solar radiation—heating up the surface of the pool and by groundwater supplying cold water to the bottom of the pool. Incident short wave radiation provides the largest energy source for heating up pool water; sensible heat flux is a much smaller energy source. Cold water entering the bottom of the pool from groundwater discharge increases the temperature and density gradients between the top and bottom of the pool. The DOC concentration in the water column dictates how much energy is absorbed near the surface and how much is transmitted to the bottom of the pool. Higher DOC concentration results in more light absorption at the pool surface and less radiation transmitted to the bottom of the pool. Finally, stream flow must enter the pool in a manner such that turbulent forces do not destroy the pool stratification. Low stream velocities result in high Richardson numbers and stratification stability. Nighttime mixing of the pool is the result of the pool cooling from LW_{emi} and *LE*; stream and groundwater input also continue to introduce relatively cool water at night.

Stream Flow

Stream flow into the pool and its momentum can destabilize the pool, resulting in mixing. Stream velocities associated with the deep channel section (Figure 3a) measured adjacent to the SM cluster are below the velocity thresholds required to destabilize the pool. On the other hand, velocities associated with the shallow channel section (Figure 3b) are below the threshold determined for July 10, 2008, but the maximum velocity associated with the shallow channel reach exceeds the velocity threshold for July 11, 2008. Stream velocities for the associated reaches were determined assuming that all of the measured flow moved through the delineated channel cross section. When the stream channel is poorly defined in the meadow (e.g., at the shallow channel stream cross section), surface water flow tends to disperse over the meadow surface like a stream overtopping its banks. The range of stream velocities determined suggests that both conditions that promote pool stratification and, depending on location, conditions that destabilize the pools exist in the meadow.

Stream flow into the pool can also affect stratification due to the temperature of the stream water entering the pool. Incoming stream and pool vertical profile temperatures on July 10, 2008 are presented in Figure 7—note that these data represent the most complete time series - when both the DTS and Tidbits were deployed. Stream temperature is cooler than the top two measured pool temperatures for the duration of the day. Stream temperature is cooler than the pool temperatures measured at 20 and 40 cm above the bottom of the pool until mid-morning and cooler than the pool temperature measured at 60 cm above the pool bottom until 14:30. Stream temperature is then warmer than these layers until 16:30, 20:00, and 22:30 at heights 60, 40 and 20 cm, respectively. Figure 7 shows that when stream temperature cools to the temperature of the pool at a given height, temperature rises at the height above the stream temperature; this suggests that once the stream mixes with a given layer, the turbulence introduced also allows that layer of the pool to mix with some of the warmer water above it. The stream channel leaving the pool is poorly defined and surface water leaving the pool comes from the surface layer. This effect of water cooler than the surface layers entering the pool coupled with surface water leaving the pool results in a net loss of energy from the pool due to advection from the stream.

Groundwater Discharge

Previous studies of thermally stratified stream pools in the Sierra Nevada and other locations of California indicate that influx of cold water, by seepage or groundwater discharge, is imperative for perpetuating cold water reservoirs in the stream pools (Nielsen, 1994; Matthews *et al.*, 1994; Matthews and Berg, 1997). While these studies suggest the importance of cold water influx, they do not report measured groundwater fluxes. We are able to quantify groundwater discharge rates in Long Meadow. LP-33 is located in the meadow center where we show significant groundwater discharge in both the summer and fall; Westside pool did not exhibit stratification—this may be, in part, because Westside pool is located at the meadow edge where groundwater exhibits a recharge signal.

Energy Balance

LP-33 heats up and stratifies during the day when net solar radiation and air temperatures increase; the pool cools and mixes after the sun sets and air temperatures decrease. Peak incoming shortwave radiation was 946 W m^{-2} on July 11, 2008—this is similar to values measured by Sadro *et al.* (2011) at nearby Emerald Lake. Where sunlight is not impeded by canopy (i.e. shaded), more solar radiation is available for heating of the water than under forest canopy. Canopy insolation from solar loading can be the most important factor in determining maximum daily stream temperature in mountain streams (Danehy *et al.*, 2004). Garner *et al.* (2012) show that a stream reach in a treeless heather moorland in Scotland (~57°N latitude) receives more net radiation and loses more latent heat than a stream reach in the adjacent woodland. Long Meadow, though lower in latitude (~37°N latitude) than the Scottish moorlands, is similar in that there are few trees to obstruct the stream from solar radiation. A comparison of net solar radiation measured at the Wolverton meteorological station and the micrometeorological station is shown in Figure 2. Both stations show similar peak net solar radiation of approximately 675 W m^{-2}. Wolverton meteorological station exhibits reduced net radiation values in the morning and evening due to shading from the canopy.

The attenuation of radiation incident to the pool surface affects how much solar energy is available for absorption at any given depth for heating the water in the pool. Other than water itself, DOC—in the form of humic and fulvic acids— has been shown to be the principal factor in the attenuation of ultra violet and PAR through the water column (Kirk, 1994; Buckaveckas and Robbins-Forbes, 2000). DOC concentrations in streams and rivers vary from 0.5 to 50 mg L^{-1} in most natural stream systems (Mullholland, 2002). Streams in catchments with larger percentage wetland area show higher DOC levels than those in similar catchments with lower percentage of wetland area (Laudon *et al.*, 2011; Gorham *et al.*, 1998). The results from DOC analysis show that samples collected from the meadow pools, stream, and outlet had consistently higher DOC levels (4.25-5.35 mg L^{-1}) compared to samples collected in Wolverton Creek, where surface water enters the meadow, or in the meadow well. The meadow well is located in the meadow-forest transition and is proximal to Wolverton Creek (Figure 1)—samples collected at this location are likely not representative of groundwater in the meadow. While the measured values are all on the low end of the range reported by Mullholland (2002) even the small difference between the lowest measured value (2.67 mg L^{-1} in Wolverton Creek) and the highest measured value (5.35 mg L^{-1} in a meadow pool) can result in a significant difference in the amount of light absorbed near the pool surface and the amount that penetrates to the bottom of the pool. Sadro *et al.* (2011) studied nearby Emerald Lake and reported average DOC concentrations of 0.78 to 0.90 mg L^{-1} and PAR attenuation coefficients of 0.27 to 0.32 m^{-1}. Laurion *et al.* (2010) observed thermal stratification in thermokarst thaw ponds in the Canadian Subarctic and Arctic—these ponds are similar in size (1-3 m diameter) and exist in systems with active peat layers. Laurion *et al.* (2010) reported DOC concentrations of 1.5-20.8 mg L^{-1} and attribute thermal stratification in their study to high attenuation of light due to high DOC and suspended solids concentrations. Deshpande *et al.* (2015) also observed thermal stratification in permafrost thaw lakes in the Canadian subarctic—DOC concentrations reported in this study range from 2.7-14.8 mg L^{-1}. Meadow pools had an average DOC concentration of 4.83 mg L^{-1} and a PAR attenuation coefficient—measured on September 25, 2015—of 1.2 m^{-1}.

Light attenuated in the water column was calculated using the Lambert-Beer's law:

(6) $$I_x = I_o e^{-K_d x}$$

where I_x is the intensity of the PAR transmitted at depth, x, I_o is the intensity of PAR that penetrates the surface of the pool (at zero depth), and K_d is the measured attenuation coefficient, 1.2 m^{-1}. The PAR attenuated by the water column between the surface and a depth x, I_a, is then:

(7) $$I_a = I_o - I_x$$

Attenuation for the K_d values determined in this study and by Sadro *et al* (2011), as a fraction of incident PAR, is presented in Figure 8—we use values from Sadro *et al.* (2011) as a comparison to other K_d values measured nearby Long Meadow. Attenuation coefficients presented by Sadro *et al.* (2011) result in 65-70% of the incident PAR reaching the bottom of the pool whereas the attenuation coefficient determined for Long Meadow results in only 20% of the incident PAR reaching the pool bottom. The same amount of PAR absorbed by the water column using the Sadro *et al*. (2011) coefficients is absorbed in the top 30-35 cm in the water column using the coefficient determined for Long Meadow. More light is absorbed at the surface of pools with elevated DOC concentrations and less light is transmitted through the water column, resulting in a greater temperature discrepancy between the surface and bottom of the pool. We hypothesize that in a Sierra meadow, where productivity can be high; the presence of organic matter in the water column may significantly affect the attenuation of incoming solar radiation and be a significant parameter in pool stratification behavior.

The energy absorbed by the top 10 cm of the pool (I_T) can be calculated on an hourly time step from the change in pool temperature as measured by the temperature logger in nearest the pool surface:

(8) $$I_T = 0.10 \rho_w \Delta T C_W$$

where ΔT is the change in temperature measured by the temperature logger nearest the pool surface and C_w is the specific heat of water. The net energy balance for the top 10 cm of the pool was calculated by summing the terms of the energy balance calculations; equation 3 was used for *LE* in this analysis. *SW* absorbed by the top ten centimeters was calculated by subtracting the SW_{out} from SW_{in} and parsing the remainder into PAR and not PAR; PAR is assumed to be 43% of incoming SW radiation—PAR absorbed by the top ten cm was calculated using equations 6 and 7. The energy balance for the top 10 cm of the pool and the energy absorbed by the top 10 cm of the pool are presented in Figure 9. The top layer of the pool starts absorbing energy just after 5 am but the energy balance does not indicate a positive energy flux into the pool until just after 09:00; we attribute this phase shift to the location of the micrometeorological station relative to

LP-33. While these locations are only about 35 meters apart, the micrometeorological station is located closer to the eastern edge of the meadow—this likely results in the station being shaded longer by the adjacent forest in the morning than LP-33. This is consistent with the more westerly pool starting to cool off before the energy balance for the top 10 cm goes negative—the lag time for the afternoon discrepancy is less than that of the morning. The peak energy input is similar for the energy absorbed (180 w m^{-2}) and the top 10 cm energy balance (213 W m^{-2}). The energy balance component exhibits a much larger cooling at the surface than the energy absorbed component.

The main driver of nighttime mixing is radiative cooling, LW_{emi}. Sadro *et al.* (2011) show that net long wave radiation is a much larger heat loss term then LE at night. Nighttime incoming long wave radiation must be low in order for emitted long wave from the pool surface to be enough to cool the pool and allow mixing. Average nighttime incoming longwave radiation averages 58 W m^{-2}—this is comparable in magnitude to average nighttime incoming long wave radiation measured in five other meadows where 4 component radiation was measured as part of the USFS Meadows Project (Table 1). Lack of canopy insolation, as described above, and low cloud cover, allows emitted long wave radiation to cool and mix LP-33 at night.

Stream residence time

A significant consequence of this stratification is that the effective “volume” of the stream, and therefore residence time of the water in the stream varies diurnally. We observed five meadow pools that exhibited stratification over an approximately one kilometer reach of stream. Pools were 1 m wide, 1-4 m long and 1-1.3 m deep. Assuming average pool dimensions, a single pool has almost 3 m^3 of volume; five pools of average size comprise approximately 15 m^3 of water. Measured stream channels in the meadow were on the order of 0.10 m wide and 0.10 m deep. Over a 1 km reach, a channel with these dimensions would hold a volume of 10 m^3. When the pools are completely mixed and the entire volume is active with stream flow, the total active volume of the stream along this reach is 25 m^3. If the pools are stratified to any degree, and only the top of part of the pool interacts with stream flow, then the active volume of the stream is reduced. For example, if the bottom half each of the pools is separated from stream flow due to thermal stratification, then the active volume of the stream is reduced by 30%. The stratification status of the pools has the potential to affect tracer tests or residence time calculations. For example, tracer tests in streams are often used to characterize interaction between the hyporheic zone and the stream (McDonnell *et al.*, 1991; Harvey and Wagner, 1996; Wagner and Harvey, 1997; Goosef *et al.*, 2003; Ward *et al.*, 2014). A key parameter in this relationship is the volume of water over the experimental stream reach. Stratified pools within the experimental reach can potentially reduce the effective stream volume and skew the relationship between the stream and hyporheic zone.

CONCLUSIONS

Polymictic pool behavior was observed in several pools in Long Meadow, Sequoia National Park California; and a more intensive investigation was carried out in a single pool, LP-33, to comprehend the processes that drive pool stratification. Incoming shortwave radiation was the primary energy source for heating pool water; sensible heat flux was a minor term. Nighttime long wave radiation, emitted from the pool surface, was the primary cooling mechanism—nighttime cooling resulted in isothermal vertical profiles. Elevated DOC in the water column, as compared to Wolverton Creek or Emerald Lake, results in greater PAR attenuation; this allows more energy to be absorbed near the pool surface and prevents more light from reaching the bottom of the pool. Stream flow into the pool introduces turbulence and can effectively cool the pool by introducing relatively cold water. Groundwater input into the bottom of the pool increases the density stratification and stability. The results from this study produced a conceptual model based on the meadow conditions that were conducive to pool stratification. This conceptual model will be useful when considering these parameters and the potential for stratification and conducting stream studies. For example, in relatively small streams, where a significant volume of water resides in stream pools, stratification can affect the active stream volume. This is an important consideration when considering parameters like stream water residence times and hyporheic-stream exchange processes.

ACKNOWLEDGEMENTS

This research was supported by the US National Science Foundation, through the Southern Sierra Critical Zone Observatory (EAR-0725097) and a Major Research Instrumentation Grant (EAR-0619947). Additional instrument support was provided by the CTEMPs facility (EAR-1128999). We would like to thank the three anonymous reviewers for their constructive criticism and helpful feedback. Thank you to Dr. Sally MacIntyre for communication with the lead author regarding energy balance and light attenuation analyses. The authors are grateful to Dr. Thomas Harmon and Dr. Henry Pai for use of their underwater PAR sensor. We would like to thank Craig Clements, Brad Esser, Roger Bales, Jan Hopmans, Robert Rice, Peter Hartsough, Armen Malazian, Mike Singleton, Matt Meadows, Adrian Rojas, Sean Kelly, and Peter Kirchner for fieldwork and laboratory assistance.

REFERENCES

Adams, E. E., Cosler, D.J., & Helfrich, R. (1990). Evaporation From Heated Water Bodies: Predicting Combined Forced Plus Free Convection. *Water Resources Research*, *26*(3), 425–435.

Allen, R. G., Pereira, L. S., Raes, D., & Smith, M. (1998). Crop evapotranspiration-Guidelines for computing crop water requirements-FAO Irrigation and drainage paper 56. *FAO, Rome*, *300*, 6541.

Bormans, M., & Webster, I. T. (1998). Dynamics of temperature stratification in lowland rivers. *Journal of Hydraulic Engineering*, *124*, 1059.

Bukaveckas, P. A., & Robbins-Forbes, M. (2000). Role of dissolved organic carbon in the attenuation of photosynthetically active and ultraviolet radiation in Adirondack lakes. *Freshwater Biology*, *43*(3), 339–354.

Chartrand, S. M., & Whiting, P. J. (2000). Alluvial architecture in headwater streams with special emphasis on step–pool topography. *Earth Surface Processes and Landforms*, *25*(6), 583-600.

Danehy, R. J., Colson, C. G., Parrett, K. B., & Duke, S. D. (2005). Patterns and sources of thermal heterogeneity in small mountain streams within a forested setting. *Forest Ecology and Management*, *208*(1–3), 287–302. doi:http://dx.doi.org/10.1016/j.foreco.2004.12.006

Dingman, S. L. (2015). *Physical hydrology*. Waveland press.

Fetter, C. W. (1994). *Applied hydrogeology* (Vol. 691). Prentice Hall Upper Saddle River.

Fischer, H. B., List, E. J., Koh, R. C. Y., Imberger, J., & Brooks, N. H. (1979). *Mixing in Inland and Coastal Waters*. Academic Press, Inc.

Garner, G., Hannah, D. M., Malcom, I. A., & Sadler, J. P. (2012). Inter-annual variability in spring-summer stream water temperature microclimate and heat exchanges: a comparison of forest and moorland environments. In *British Hydrological Society Eleventh National Symposium, Hydrology for a changing world, Dundee*.

Gooseff, M. N., Wondzell, S. M., Haggerty, R., & Anderson, J. (2003). Comparing transient storage modeling and residence time distribution (RTD) analysis in geomorphically varied reaches in the Lookout Creek basin, Oregon, USA. *Advances in Water Resources*, *26*(9), 925–937. doi:10.1016/S0309-1708(03)00105-2

Gorham, E., Underwood, J. K., Janssens, J. A., Freedman, B., Maass, W., Waller, D. H., & Ogden, J. G. (1998). The chemistry of streams in southwestern and central Nova Scotia, with particular reference to catchment vegetation and the influence of dissolved organic carbon primarily from wetlands. *Wetlands*, *18*(1), 115–132.

Harvey, J. W., Wagner, B. J., & Bencala, K. E. (1996). By Was S); Hyporheic Exchange Persisted When Base Flow Was Decreasing By. *Water Resources*, *32*(8), 2441–2451.

Hausner, M. B., Suárez, F., Glander, K. E., Giesen, N. Van De, Selker, J. S., & Tyler, S. W. (2011). Calibrating Single-Ended Fiber-Optic Raman Spectra Distributed Temperature Sensing Data. *Sensors*, *11*, 10859–10879. doi:10.3390/s111110859

Hicks, B. B. (1972). Some evaluations of drag and bulk transfer coefficients over water bodies of different sizes. *Boundary-Layer Meteorology*, *3*(2), 201–213. doi:10.1007/BF02033919

Horne, A. J., & Goldman, C. R. (1994). *Limnology*. McGraw-Hill New York.

Howard, L. N. (1961). Note on a paper of John W. Miles. *J.Fluid Mech*, *10*(4), 509–512.

Huntington, G. L., & Akeson, M. A. (1987). Soil resource inventory of Sequoia National Park, central part, California. *University of California, Merced Library*.

Kattelmann, R., & Embury, M. (1996). Riparian areas and wetlands. In *Sierra Nevada Ecosystem Project, Final Report to Congress* (Vol. 3).

Kirk, J. T. O. (1994). *Light and photosynthesis in aquatic ecosystems*. Cambridge university press.

Laudon, H., Berggren, M., Ågren, A., Buffam, I., Bishop, K., Grabs, T., … Köhler, S. (2011). Patterns and dynamics of dissolved organic carbon (DOC) in boreal streams: The role of processes, connectivity, and scaling. *Ecosystems*, *14*(6), 880–893.

Lisle, T. E. (1987). Pool Depths Independently of Discharge. Res. Note PSW-RN-394. Berkeley, CA: U.S. Department of Agriculture, Forest Service, Pacific Southwest Forest and Range Experiment Station. 4 p

Loheide II, S. P., Deitchman, R. S., Cooper, D. J., Wolf, E. C., Hammersmark, C. T., & Lundquist, J. D. (2009). A framework for understanding the hydroecology of impacted wet meadows in the Sierra Nevada and Cascade Ranges, California, USA. *Hydrogeology Journal*, *17*(1), 229–246.

MacIntyre, S., Romero, J., & Kling, G. W. (2002). Spatial-temporal variability in surface layer deepening and lateral advection in an embayment of Lake Victoria, East Africa. *Limnology and Oceanography*, *47*(3), 656–671. doi:10.4319/lo.2002.47.3.0656

Matthews, K. R., & Berg, N. H. (1997). Rainbow trout responses to water temperature and dissolved oxygen stress in two southern California stream pools. *Journal of Fish Biology*, *50*(1), 50–67.

Matthews, K. R., Berg, N. H., Azuma, D. L., & Lambert, T. R. (1994). Cool water formation and trout habitat use in a deep pool in the Sierra Nevada, California. *Transactions of the American Fisheries Society*, *123*(4), 549–564.

McDonnel, J.J., Stewart, M.K., and I.F. Owens, I. F. (1991). Subsurface. *Water Resources Research*, *27*(12), 3065–3073.

Miles, J. W. (1961). On the stability of heterogeneous shear flows. *J.Fluid Mech*, *10*(4), 496–508.

Mulholland, P. J. (2002). *Large-scale patterns in dissolved organic carbon concentration, flux, and sources*. Academic Press/Elsevier Science: New York.

Nielsen, J. L., Lisle, T. E., & Ozaki, V. (1994). Thermally stratified pools and their use by steelhead in northern California streams. *Transactions of the American Fisheries Society*, *123*(4), 613–626.

O'Donnell, T. (2012). Evaluation of stream temperature spatial variation using distributed temperature sensing. Ph. D. Dissertation, Oregon State University

Purdy, S. E., & Moyle, P. B. (2006). Mountain Meadows of the Sierra Nevada. M. Sc. Thesis University of California, Davis

Ratliff, R. D., & Forest, P. S. (1985). *Meadows in the Sierra Nevada of California: state of knowledge* (Vol. 84). US Dept. of Agriculture, Forest Service, Pacific Southwest Forest and Range Experiment Station.

Rogers, A. S. (1958). Physical behavior and geologic control of radon in mountain streams. *In Experimental and Theoretical Geophysics, U.S. Geological Survey Bulletin 1052-E*, 187–212.

Sadro, S., Melack, J. M., & MacIntyre, S. (2011). Depth-integrated estimates of ecosystem metabolism in a high-elevation lake (Emerald Lake, Sierra Nevada, California). *Limnology and Oceanography*, *56*(5), 1764–1780. doi:10.4319/lo.2011.56.5.1764

Selker, J., Van De Giesen, N., Westhoff, M., Luxemburg, W., & Parlange, M. B. (2006). Fiber optics opens window on stream dynamics. *Geophys.Res.Lett*, *33*(24), 24401.

Service, N. P. (2014). Vegetation Inventory Project for Sequoia and Kings Canyon National Parks. 2001-2014. Project-2173101. Project. Retrieved March 11, 2015, from http://science.nature.nps.gov/im/inventory/veg/project.cfm?ReferenceCode=2173101

Shaw, G. D. (2009). Investigating groundwater and surface water interactions using novel isotopes and geochemical tracers in the upper Merced River Basin, Sierra Nevada, California. Ph. D. Dissertation, University of California, Merced

Szabo, Z., & Zapecza, O. S. (1991). Geologic and geochemical factors controlling uranium, radium-226, and radon-222 in ground water, Newark Basin, New Jersey. *Field Studies of Radon in Rocks, Soils, and Water*, 243–266.

Tate, K. W., Lancaster, D. L., & Lile, D. F. (2007). Assessment of thermal stratification within stream pools as a mechanism to provide refugia for native trout in hot, arid rangelands. *Environmental Monitoring and Assessment*, *124*(1), 289–300.

Tyler, S. W., Selker, J. S., Hausner, M. B., Hatch, C. E., Torgersen, T., Thodal, C. E., & Schladow, S. G. (2009). Environmental temperature sensing using Raman spectra DTS fiber-optic methods. *Water Resources Research*, *45*(4).

Wagner, B. J., & Harvey, J. W. (1997). Experimental design for estimating parameters of rate-limited mass transfer: Analysis of stream tracer studies. *Water Resources Research*, *33*(7), 1731. doi:10.1029/97WR01067

Wahrhaftig, C., Moore, J. G., & Tinsley, J. C. (1984). *Geomorphology and Glacial Geology, Wolverton and Crescent Meadow Areas and Vicinity, Sequoia National Park, California*. US Department of the Interior, Geological Survey.

Ward, A. S., Gooseff, M. N., Fitzgerald, M., Voltz, T. J., & Singha, K. (2014). Spatially distributed characterization of hyporheic solute transport during baseflow recession in a headwater mountain stream using electrical geophysical imaging. *Journal of Hydrology*, *517*, 362–377. doi:10.1016/j.jhydrol.2014.05.036

Whitaker, J. G., & Jaeggi, M. N. (1982). Origin of step-pool systems in mountain streams. *Journal of Hydraulics Division, Proc. of ASCE, 108*(HY6), 758–773.

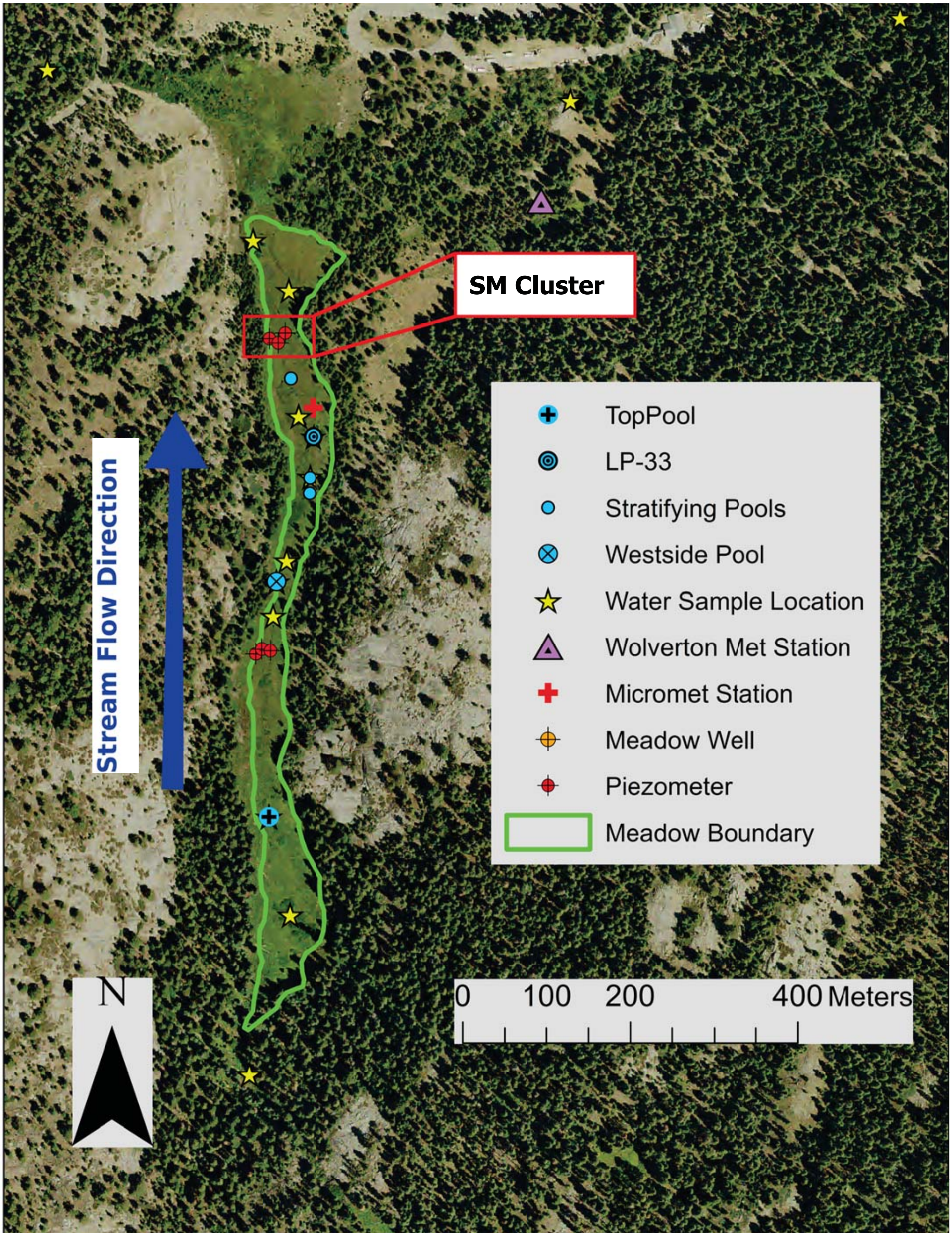

Figure 1—Site Map for Long Meadow, Sequoia National Park, CA.

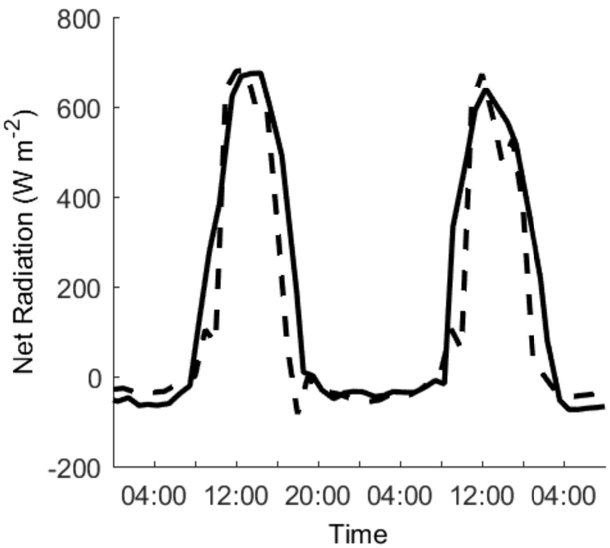

Figure 2—Net radiation measured at the micrometeorological station and the Wolverton meteorological station for July 10-11, 2008.

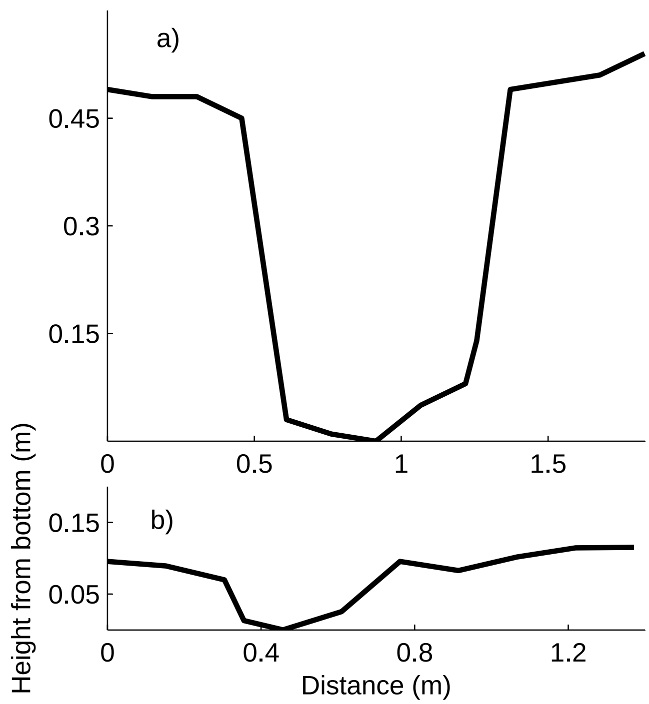

Figure 3—Stream cross sections measured at two locations in the meadow stream and adjacent to the SM cluster. Cross sections were measured perpendicular to stream flow.

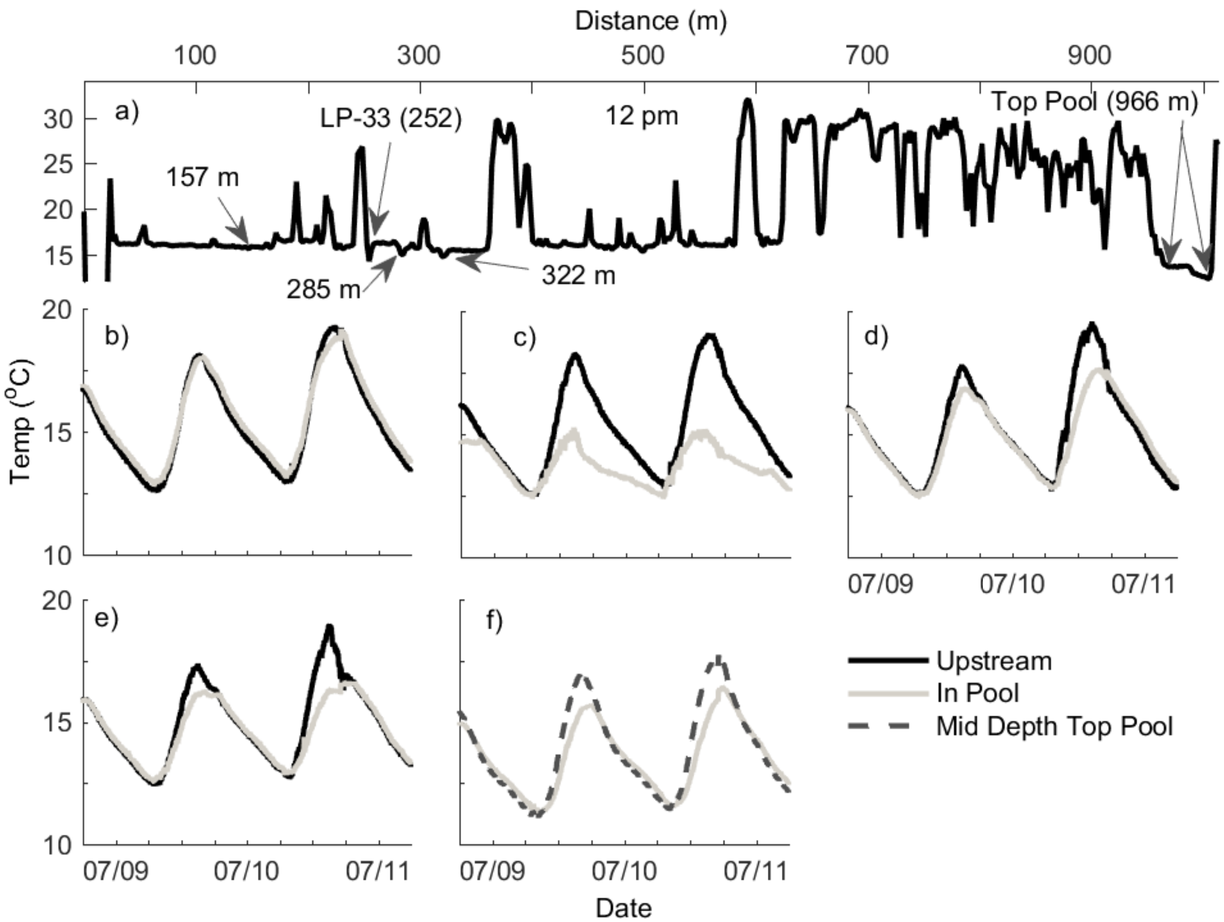

Figure 4—Stream and pool temperatures measured by the DTS system including a longitudinal stream trace captured at 12:00 on July 10, 2008 (a); upstream and in pool temperatures measured from July 9-11, 2008 at pools located at stream distances 157 m (b), 252 m (c)–this pool also referred to as LP-33, 285 m (d) and 322 m (e); in pool and mid depth of pool coils at stream distance 966 (f)—this pool is also referred to as Top Pool. Stream distances for the pools represented in panels (b)-(f) are indicated with gray arrows in panel (a). Cable not placed in the stream is indicated by temperatures that are significantly higher than stream temperatures in panel (a).

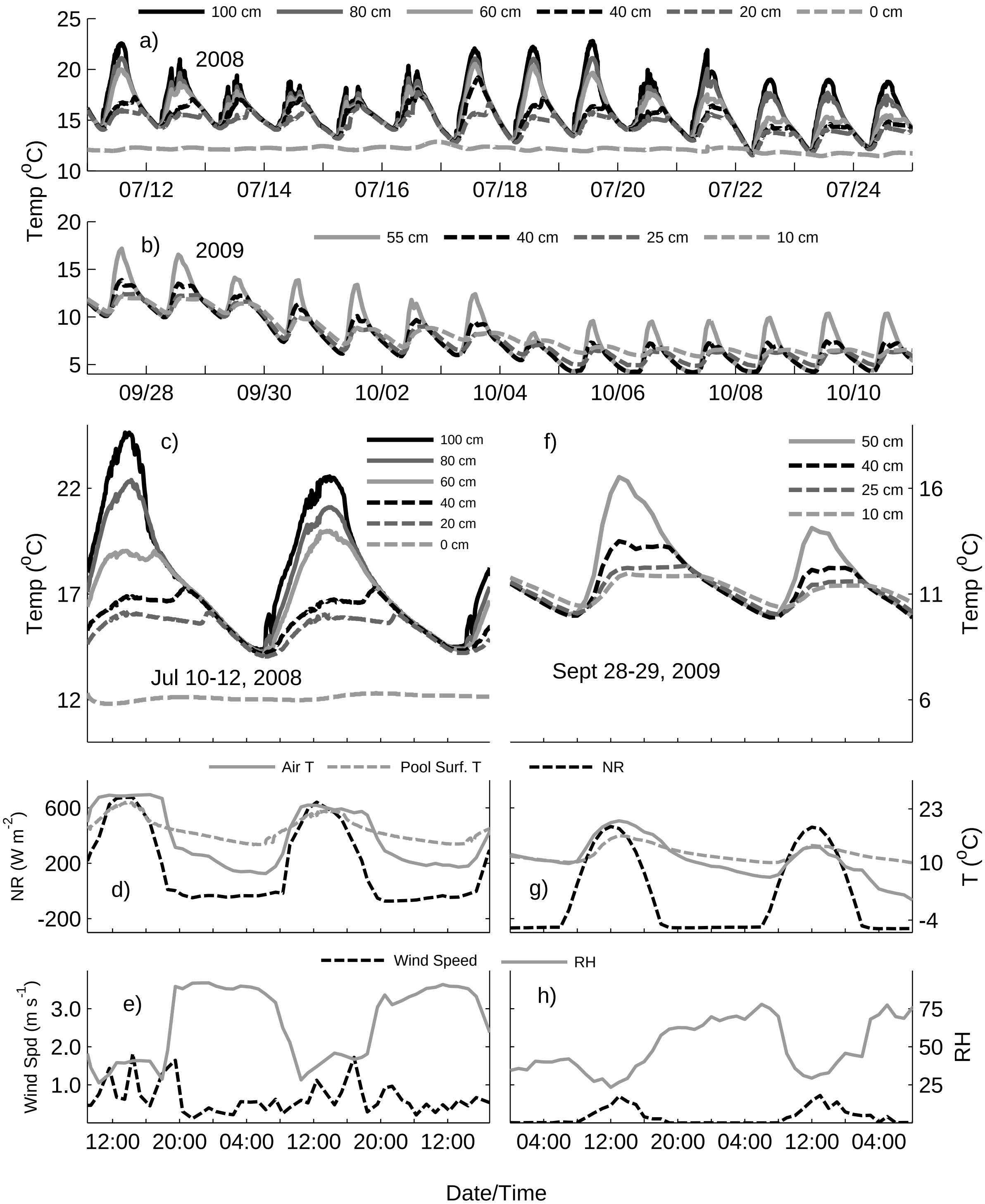

Figure 5--Vertical temperature profiles measured with temperature loggers for July 12-24, 2008 (a); September 28-October 10, 2009 (b). A 2-day representation of LP-33 vertical temperature profile is plotted for July 10-12, 2008 in panel (c); surface water temperature measured by the temperature logger nearest the pool surface, as well as air temperature and net radiation measured by the micrometeorological station are plotted in panel (d); wind speed and relative humidity measured at the micrometeorological station are plotted in panel (e). A 2-day representation of LP-33 vertical temperature profile is plotted for September 28-29, 2009 in panel (f); surface water temperature measured by the temperature logger nearest the pool surface air temperature measured at the Wolverton met station and net radiation calculated using methods described by Allen et al. (1998) are plotted in panel (g); wind speed and relative humidity measured at the Wolvertone meteorological station are presented in panel (h).

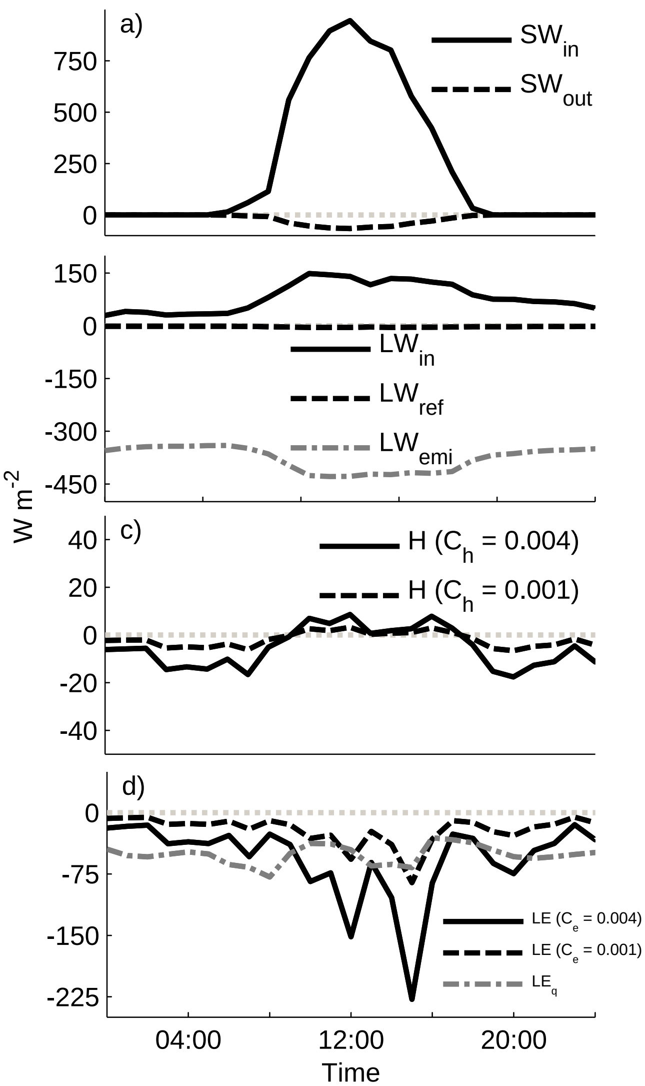

Figure 6—Energy balance terms calculated for July 11, 2008. Terms include Shortwave radiation in and out (a); Long wave radiation in, reflected, and emitted (b); sensible heat flux (c); and latent heat flux (d). Zero line is plotted as light gray dotted line.

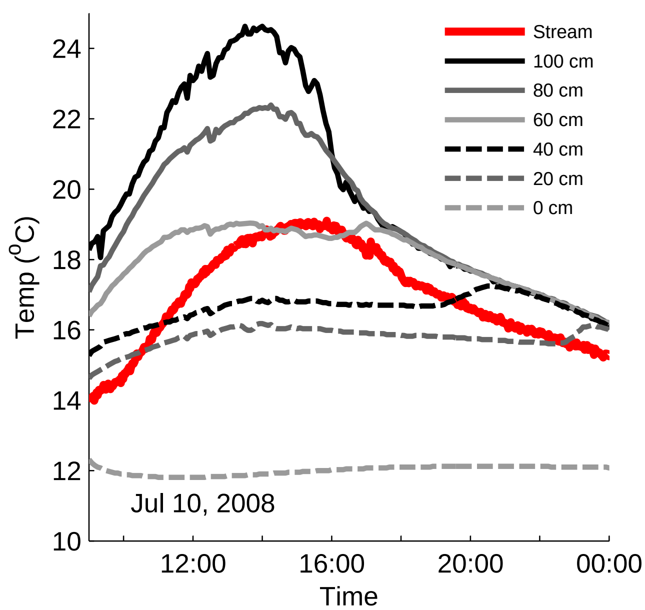

Figure 7—Vertical temperature profile for LP-33 on July 10, 2008 plotted with stream temperature measured just upstream of the pool with the DTS system.

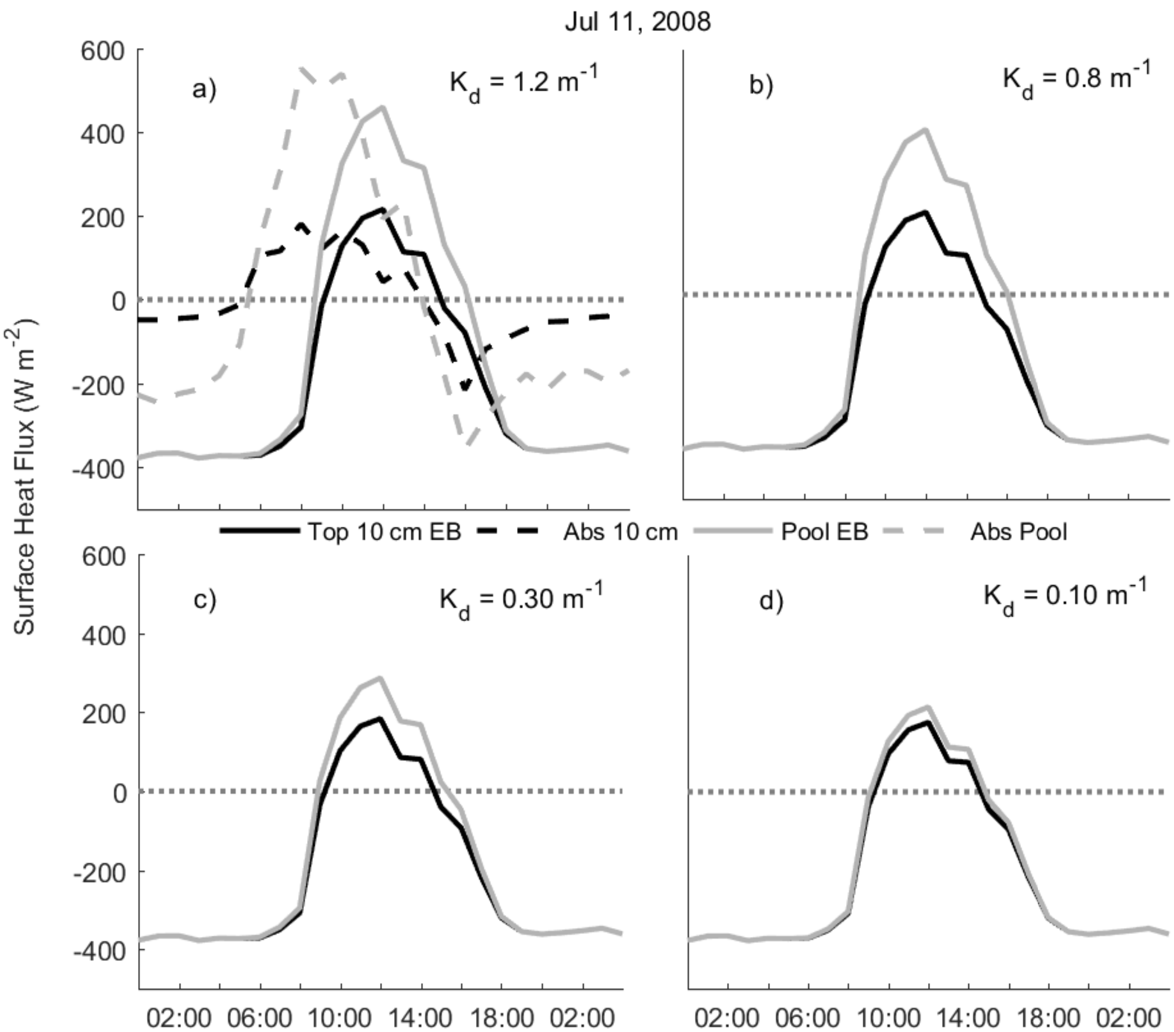

Figure 8—Energy balance calculated for the top 10 cm and for the entire vertical profile of the pool are plotted in all four panels. Energy absorbed in the top 10 cm and for the entire depth of the pool, as measured by the associated temperature loggers, for July 11, 2008 are included in panel (a). Calculations for panel (a) use Kd measured in Long Meadow; calculations in panel (b) use a reduce Kd, panels (c,d) use the light attenuation coefficient range presented by Sadro et al (2011)

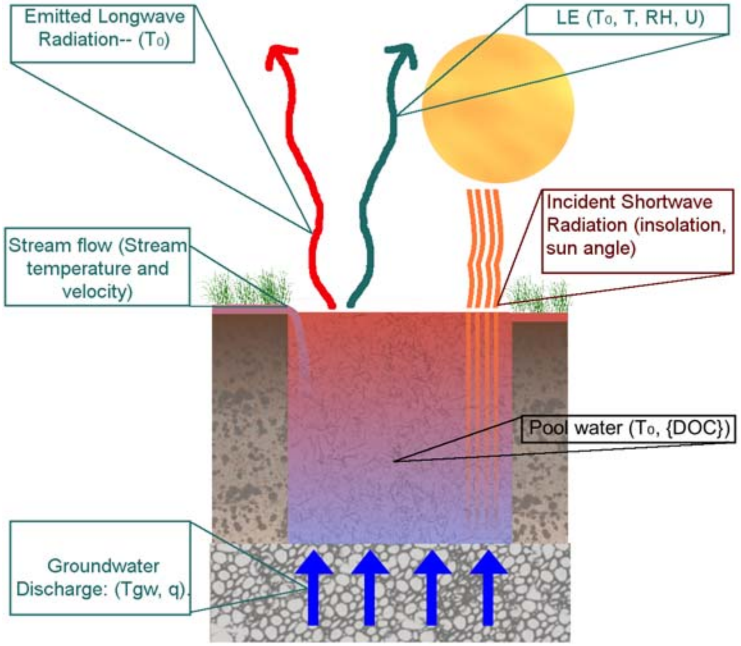

Figure 9—Conceptual model of parameters that drive meadow pool stratification; variables that determine the strength of each parameter in parentheses.

Table 1—Saturated hydraulic conductivity, average Darcy velocity (from deep to mid piezometers) and groundwater temperature at the meadow edge, slope, and center for July 17-18 and September 28-29, 2009.

		July-09		September-09	
Location	**K_s (m s^{-1})**	**Darcy Velocity (m s^{-1})**	**Temperature (°C)**	**Darcy Velocity (m s^{-1})**	**Temperature (°C)**
Meadow Edge	$1.98 \cdot 10^{-5}$	$-4.23 \cdot 10^{-6}$	6.32-7.83 ±0.05	$-6.20 \cdot 10^{-6}$	8.44-8.54 ±0.05
Meadow Slope	$2.06 \cdot 10^{-6}$	$3.58 \cdot 10^{-7}$	6.39-8.24 ±0.05	$1.50 \cdot 10^{-7}$	9.15-9.39 ±0.05
Meadow Center	$1.13 \cdot 10^{-5}$	$9.38 \cdot 10^{-7}$	5.89-6.93 ±0.05	$3.70 \cdot 10^{-6}$	7.75-8.00 ±0.05

Table 2—Mean and standard deviation of DOC concentrations for various meadow sample types; standard deviation provided where more than two samples at a given location type were collected.

Sample Location	**Mean DOC (mg L^{-1})**	**Standard Dev (mg L^{-1})**
Meadow Pools	4.83	0.30
Meadow Inlet	3.05	--
Meadow Stream	3.09	--
Meadow Outlet	5.25	--
Wolverton Creek	2.46	0.39

Table 3—LP-33 temperatures and water densities used in Richardson number calculations.

Date	Surface T (°C)	Surface Water ρ (kg m^{-3})	T 20 cm (°C)	20 cm Water ρ (kg m^{-3})
July 10, 2008	24.58	997.15	22.32	997.70
July 11, 2008	22.54	997.65	21.08	997.98

Table 4—Average nighttime incoming long wave radiation measured in 6 meadows in the Sierra Nevada and calculated in Long Meadow.

Location	**Latitude (N)**	**Longitude (W)**	**Elevation**	**Ave night time** LW_{in} **(W m^{-2})**
Big Flat	40.148463	120.460241	1735	80
Cook House	38.791129	120.007665	2140	86
Faust Cabin	38.046078	120.11346	1610	108
Middle Perazzo	39.492426	120.351376	1970	118
Trout Creek	38.912359	119.970518	1910	79
Long Meadow Calc	36.592659	118.737269	2200	42
LongMeadow Measured	36.592659	118.737269	2200	58